J Solid State Electrochem (2010) 14:1697–1703
DOI 10.1007/s10008-010-1009-9

ORIGINAL PAPER

Manganese oxide thin films prepared by potentiodynamic electrodeposition and their supercapacitor performance

Ming-Tsung Lee · Jeng-Kuei Chang · Yao-Tsung Hsieh · Wen-Ta Tsai · Chung-Kwei Lin

Received: 20 November 2009 / Revised: 12 January 2010 / Accepted: 13 January 2010 / Published online: 23 February 2010

Abstract Manganese oxide film for supercapacitor applications was prepared by potentiodynamic electrodeposition in a manganese acetate plating solution. The effects of the potential sweep rate on the oxide microstructure, crystallinity, and chemical states were examined using a scanning electron microscope, an X-ray diffractometer, and an X-ray photoelectron spectrometer, respectively. Electrochemical performance of the film electrodes was evaluated using a cyclic voltammetric measurement. The experimental results indicate that the deposition potential sweep rate significantly affected the material properties of the prepared oxide films. The oxide-specific capacitance increased from 262 to 337 F/g when the sweep rate was increased from 100 to 400 mV/s. The key material factors that govern the specific capacitance and cyclic stability of the oxide electrodes were discussed.

Keywords Manganese oxide · Potentiodynamic electrodeposition · Supercapacitor performance

Introduction

Climate change and the decreasing availability of fossil fuels have forced society to move towards alternative and sustainable resources. The electricity generated from renewable energy (e.g. from the sun or wind) usually has to be stored before it is used. Supercapacitors are charge-storage devices that have a greater power density and a longer cycle life than those of batteries, and a higher energy density than that of conventional capacitors [1]. Accordingly, their applications in electric vehicles, portable electronics, medical devices, and military missile systems have been proposed. Manganese (Mn) oxide is considered as a favorable electrode material for supercapacitors due to its satisfactory electrochemical performance and its natural abundance and environmental compatibility. The charge-storage mechanism of Mn oxide in aqueous electrolytes has been proposed as follows [2, 3]:

$$\mathrm{MnO_2} + n\mathrm{C^+} + n\mathrm{e^-} \rightleftarrows \mathrm{MnO_{2-}}_n(\mathrm{OC})_n \quad (n \leq 1) \qquad (1)$$

where $\mathrm{C^+}$ denotes the protons and alkali metal cations ($\mathrm{Li^+}$, $\mathrm{Na^+}$, $\mathrm{K^+}$). The Mn oxidation state varies continuously and reversibly between the trivalent and tetravalent forms during the charge–discharge process, contributing to pseudocapacitive behavior [4, 5].

The known preparation processes for Mn oxide supercapacitor electrodes include electrodeposition [3, 6], thermal decomposition [7], co-precipitation [4, 8], sol–gel processes [9, 10], physical vapor deposition [11], and hydrothermal synthesis [12]. Different fabrication courses lead to different material characteristics and pseudocapacitive performance of the obtained Mn oxides. The advantages of using an electrochemical preparation method are simplicity, reliability, accuracy, versatility, and low cost. While potentiostatic electrodeposition is commonly used to produce Mn oxide film with capacitive properties [3, 5, 6, 9, 13], the potentiodynamic method has been rarely studied [14, 15]. Prasad and Miura [15] reported that, in a plating

M.-T. Lee · J.-K. Chang (✉) · Y.-T. Hsieh · W.-T. Tsai
Department of Materials Science and Engineering,
National Cheng Kung University,
1 University Road,
Tainan 701, Taiwan, Republic of China
e-mail: catalyst@mail.mse.ncku.edu.tw

C.-K. Lin
Department of Materials Science, Feng Chia University,
Taichang, Taiwan, Republic of China

solution consisting of $MnSO_4$, potentiodynamically deposited Mn oxide had much better charge-storage performance than that of the potentiostatically prepared one. Hu and Wang [14] found that the two deposition procedures, also from the $MnSO_4$ precursor, did not lead to significant differences in pseudocapacitance between the prepared oxide electrodes. This discrepancy requires further investigation. In Ref. [15], the authors attributed the superior capacitive performance of the potentiodynamically deposited film solely to a highly porous structure of the oxide electrode; no other detailed analytical data was presented. Nevertheless, we have recently noted that the chemically hydrous state of Mn oxide seems to be one of the most important factor that governs oxide-specific capacitance [16].

In the present study, Mn oxide film was prepared using potentiodynamic electrodeposition with various sweep rates. The plating bath was a Mn acetate solution, in which the deposition rate is higher and the deposition potential required is lower than those found in inorganic $MnSO_4$ plating solution [17]. Besides studying the surface morphology and cross-sectional microstructure of the deposited films, chemical states of the oxides were also examined. According to the analytical data, the key factors that determine the pseudocapacitive performance of Mn oxide are suggested.

Experimental methods

Mn oxide was electroplated onto graphite substrates in 0.25 M $Mn(CH_3COO)_2$ solution at 25 °C. The substrates (1 cm^2) were first polished with SiC paper, then degreased with acetone and water, etched in 0.2 M H_2SO_4, and finally washed with pure water in an ultrasonic bath. During the electrodeposition, a platinum sheet and a saturated calomel electrode (SCE) were used as the counter and reference electrodes, respectively. A previous study [18] reported that in this plating solution, anodic deposition of Mn oxide began when the applied potential exceeded 0.3 V and that a mass transfer limitation occurred beyond 0.6 V. In the present study, the potentiodynamic deposition was performed by repeatedly sweeping the potential in a region of 0–1 V using an EG&G model 263 potentiostat. Various potential sweep rates, ranging from 100 to 400 mV/s, were adopted. The weight change of the electrode before and after deposition was measured using a microbalance (with an accuracy of 10^{-5} g). The oxide loading mass was kept around 1.0–1.1 mg by controlling the sweep cycle (i.e., 40 cycles for 100 mV/s, 90 cycles for 200 mV/s, 150 cycles for 300 mV/s, and 225 cycles for 400 mV/s).

The crystal structure of the deposited films was determined using a Rigaku D/MAX-2500 glancing angle X-ray diffractometer (GAXRD). The surface morphology and cross-sectional microstructure of the electrodes were examined using a scanning electron microscope (SEM, Philip XL-40FEG). X-ray photoelectron spectroscopy (XPS) was employed to study the chemical states. The measurements were performed with a PHI 5000 Versa-Probe spectrometer using monochromated Al Kα radiation as the X-ray source.

The electrochemical properties of the oxide electrodes were characterized by cyclic voltammetry (CV) in 2 M KC1 solution at 25 °C. The CV scan rate varied from 5 to 100 mV/s. A three-electrode system, similar to that used for the electrodeposition, was adopted. The electrochemical stability of the electrodes was evaluated by repeating the CV scan (at a rate of 50 mV/s) for 500 cycles. The variation of the oxide-specific capacitance versus the cycle number was recorded.

Results and discussion

Surface morphology, cross-sectional microstructure, and crystallinity

Figure 1 (in the left column) show the surface morphologies, observed using SEM, of the oxide films potentiodynamically deposited at 100, 200, 300, and 400 mV/s, respectively. At the lower deposition sweep rate, the obtained oxide consisted of interweaving nano-sized fibers, leading to high porosity of the electrode. When the sweep rate was increased, the deposited oxide gradually became condensed, probably because the time interval between every deposition was shortened. At a rather fast sweep rate of 400 mV/s, the fiber-like feature disappeared; instead, the oxide was compact and with relatively smooth surface. The kinetics of the deposition process may be a crucial topic, which deserves further studies.

The cross-sectional microstructures of the oxide films were also examined with SEM; the micrographs are shown in the right column of Fig. 1. A layered structure was clearly recognized in the 100-mV/s-deposited oxide film. Interestingly, the layer number coincided with the cycle number for the potentiodynamic deposition, indicating that the nucleation and growth processes of Mn oxide occurred repeatedly in every deposition cycle. However, because a higher potential sweep rate did not allow enough time for new nuclei to form, newly deposited Mn oxide just grew onto the previous one; therefore, the layered structure and the inter-layer porosity were gradually eliminated as revealed in the figure. Figure 1 also shows that the film thickness decreased with increasing potential sweep rate (from ~3 μm at 100 mV/s to ~2 μm at 400 mV/s). Since the deposition mass was similar, this observation indicates

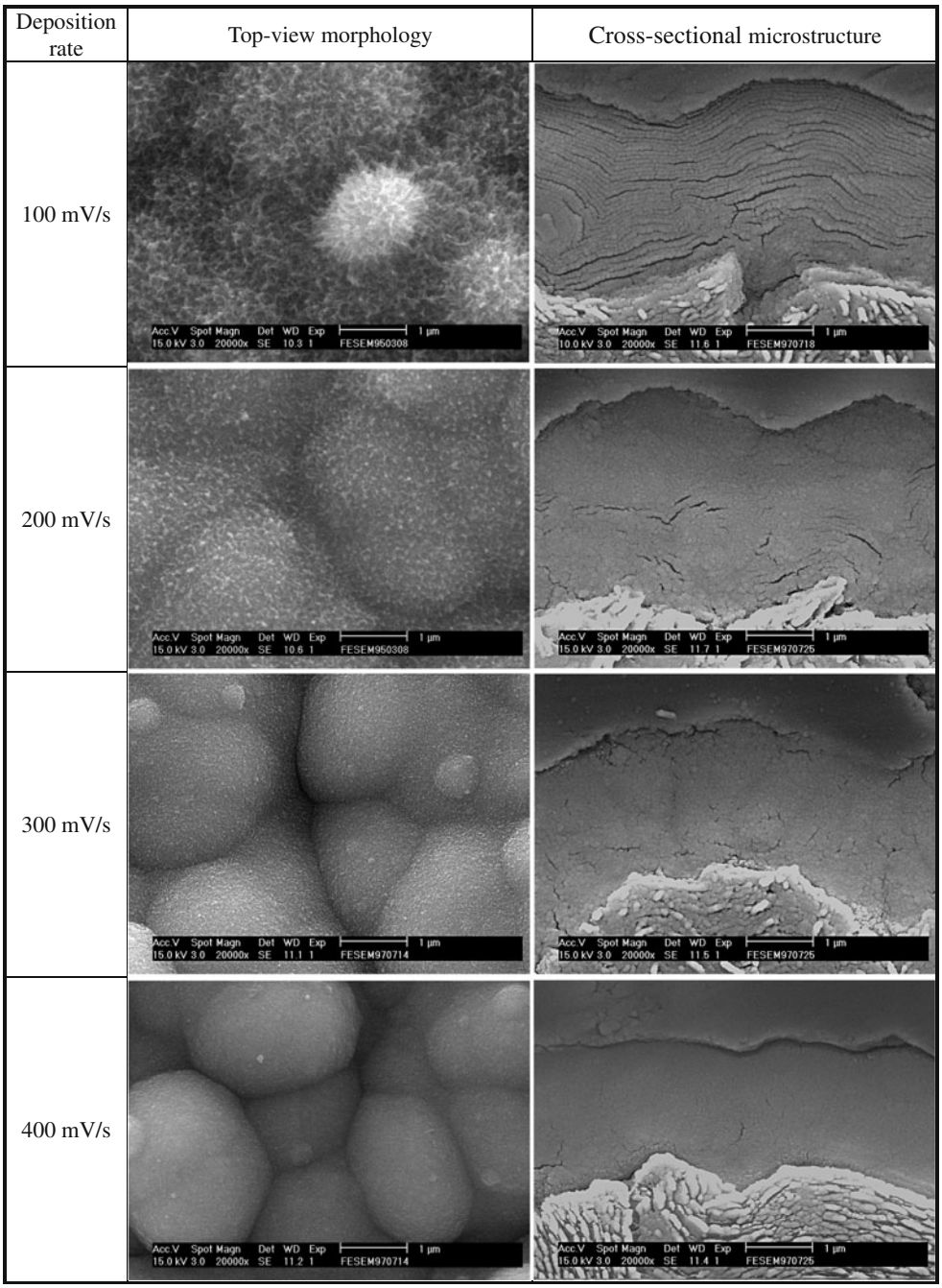

Fig. 1 SEM top-view and cross-sectional micrographs of the Mn oxide films potentiodynamically deposited at various potential sweep rates

that the apparent density of the deposited oxide increased with increasing the sweep rate. This result contradicts that reported by Prasad and Miura [15], who indicated that increasing the potential sweep rate for deposition in $MnSO_4$ solution led to higher film porosity. The chemistry of different precursors ($MnSO_4$ in [15], but $Mn(CH_3COO)_2$ in this study) seems to play an important role. However, further investigation is necessary to address this issue.

The crystal structure of the oxide films was analyzed with an X-ray diffractometer. The results (not shown here) revealed that all the potentiodynamically deposited oxides, regardless of the potential sweep rate, were highly amorphous in nature.

Chemical states

Figure 2a shows the Mn $2p_{3/2}$ XPS spectra of the Mn oxides deposited at various potential sweep rates. As illustrated, a binding energy shift, corresponding to the chemical state change, among the spectra was found. Specifically, a higher deposition sweep rate led to a lower binding energy of the Mn $2p_{3/2}$ electron, suggesting that the oxide had a lower Mn oxidation state [19]. It is known that the valence of Mn can be more precisely identified by measuring the multiplet splitting width of two Mn 3*s* XPS peaks [20]. Therefore, the spectra of this orbit were also

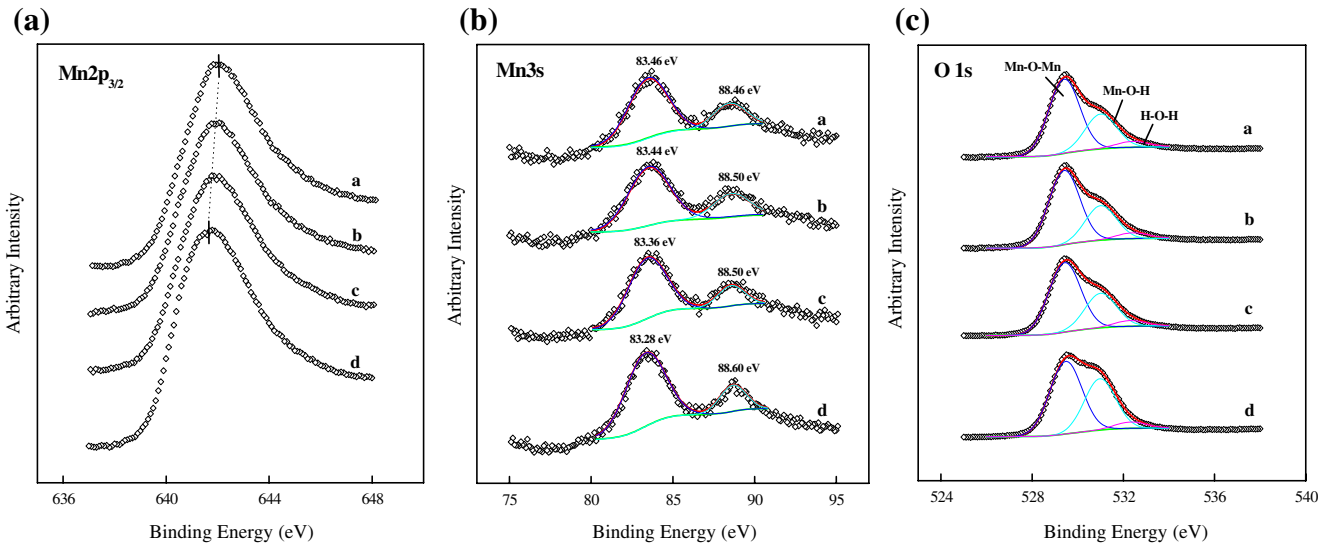

Fig. 2 XPS spectra of the **a** Mn $2p_{3/2}$ orbit, **b** Mn 3*s* orbit, and **c** O 1*s* orbit for the Mn oxide films deposited at various potential sweep rates (*curve a* 100 mV/s, *curve b* 200 mV/s, *curve c* 300 mV/s; *curve d* 400 mV/s)

acquired; the obtained data are shown in Fig. 2b. The exchange interaction between the core level electron (3*s*) and the unpaired electrons in the valence band (3*d*) results in the peak separation (ΔE) of the Mn 3*s* spectrum upon photoelectron ejection [21]. Accordingly, a lower valence of Mn results in a wider ΔE. As shown in Fig. 2b, the splitting width of the Mn 3*s* peaks increases with increasing the potential sweep rate for deposition. The peak locations, derived from Gauss-fitting results, and ΔE of the spectra are listed in Table 1. The ΔE for MnO, Mn_3O_4, Mn_2O_3, and MnO_2 reference compounds, which were reported in the literature [20], are also shown in this table for comparison. The results indicate that the deposited oxide films were composed of trivalent and tetravalent Mn; however, with increasing deposition sweep rate, the Mn oxidation state gradually approached trivalence.

The O 1*s* spectra of the various oxide films were also measured; the results are shown in Fig. 2c. As demonstrated, every spectrum can be deconvoluted into three constituent components that correspond to three oxygen-containing species, which are Mn oxide (Mn–O–Mn) at around 529.8 eV, Mn hydroxide (Mn–O–H) at around 531.0 eV, and water (H–O–H) at around 532.3 eV [20, 22], respectively. The Gauss-fitted peak areas, representing the relative content concentrations of the components, of the various deposited oxides are summarized in Table 1. As shown, the Mn–O–H to Mn–O–Mn ratio increased with increasing deposition sweep rate while the structural water (H–O–H) content remained almost constant among the oxides. Apparently, the higher the deposition sweep rate became (or the more the deposition cycle number), the more the hydrous species was involved in the deposit, although the reason was not clear yet.

Pseudocapacitive performance

Figure 3 shows the cyclic voltammograms of the various oxide electrodes measured in 2 M KCl aqueous solution with a CV scan rate of 5 mV/s. For all the CV curves, the response current essentially remained constant during forward and backward potential scans within a range of 1 V but it immediately changed its flow direction when the potential was switched to be in reverse. Moreover, the anodic and cathodic areas of the CV curves were symmetric. The quasi-rectangular CV shape, which reflects ideal pseudocapacitive behavior, is attributed to a continuously and reversibly faradic redox transition of Mn oxide over the potential range. A close comparison of the CV curves shown in Fig. 3 reveals that their enclosed areas are different, indicating a superior charge-storage capability of the oxide film deposited at the highest potential sweep rate. The specific capacitance (C) of the Mn oxide can be quantitatively evaluated according to the following equation:

$$C = Q_{\mathrm{m}}/\Delta V \tag{2}$$

where Q_{m} is the specific voltammetric charge (based on mass) integrated from both the anodic and cathodic CV scans, and ΔV is the potential scanning range. The calculated specific capacitances of the 100-, 200-, 300-, and 400-mV-deposited oxides are 262, 298, 318, and 337 F/g, respectively. Previous studies [3, 5, 6, 13, 14] indicated that the capacitances of Mn oxide prepared using potentiostatic deposition were approximately 200–250 F/g. The increase of oxide capacitance with deposition sweep rate observed in the present work is consistent with that reported by Prasad and Miura [15]. Figure 3 also indicates that an irreversible

Table 1 XPS analytical results of the Mn oxide films deposited at various potential sweep rates

	Mn 3s			O 1s	
	E_1 (eV)	E_2 (eV)	ΔE (eV)	Species	Peak area (%)
Potential sweep rate for electrodeposition					
100 mV/s	83.46	88.46	5.00	Mn–O–Mn	65%
				Mn–O–H	30%
				H–O–H	5%
200 mV/s	83.44	88.50	5.06	Mn–O–Mn	63%
				Mn–O–H	32%
				H–O–H	5%
300 mV/s	83.36	88.50	5.14	Mn–O–Mn	61%
				Mn–O–H	34%
				H–O–H	5%
400 mV/s	83.28	88.60	5.32	Mn–O–Mn	57%
				Mn–O–H	39%
				H–O–H	5%
Species					
MnO			5.79		
Mn_3O_4			5.50		
Mn_2O_3			5.41		
MnO_2			4.78		

reduction reaction occurred near 0 V for the 300- and 400-mV/s-deposited oxide electrodes. Since the oxide deposited using a higher potential sweep rate had a lower Mn oxidation state (as depicted in Fig. 2), it seemed to be less stable and tended to cathodically dissolve (to form Mn^{2+}) in the electrolyte.

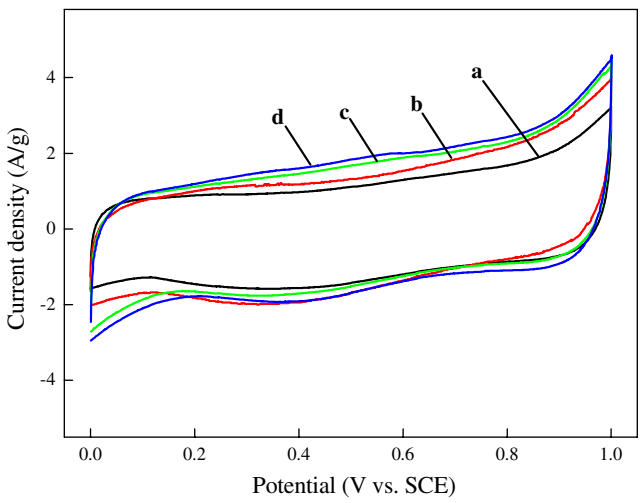

Fig. 3 Cyclic voltammograms of the Mn oxide films deposited at various potential sweep rates (*curve a* 100 mV/s, *curve b* 200 mV/s, *curve c* 300 mV/s; *curve d* 400 mV/s). The measurements were performed in 2 M KCl aqueous solution with a CV scan rate of 5 mV/s

The electrochemical performance of the oxide electrodes was recorded at various CV scan rates. It was found that even at a high measuring rate of 100 mV/s, the rectangular shapes (i.e., pseudocapacitive behavior) of the CV curves were still obtainable, indicating a satisfactory high-power performance for supercapacitor applications. Figure 4 shows the specific capacitances of the various oxide electrodes as a function of the measuring CV scan rate. Since the pseudocapacitive behavior results from the electrochemical redox reaction of Mn oxide, a monotonous decline in capacitance with increasing CV measuring rate was clearly observed due to the kinetic limitation. Moreover, the internal potential drop (or iR drop) of the electrode and diffusion limitation of reactants and products near the electrode/electrolyte interface also make the capacitance decline at the higher CV scan rates. Figure 4 shows that at a CV scan rate of 100 mV/s, approximate 60% of the capacitances measured at 5 mV/s can be maintained for all the oxide films prepared. This figure also indicates that, regardless of the CV measuring rate, a higher deposition sweep rate always led to a higher specific capacitance of the oxide film. It should be emphasized that since both the most compact oxide (in the present paper) and the most porous oxide (in Prasad and Miura's report [15]) generated the highest pseudocapacitance in its respective study, this physical issue (i.e., porosity or microstructure) does not seem to be a key

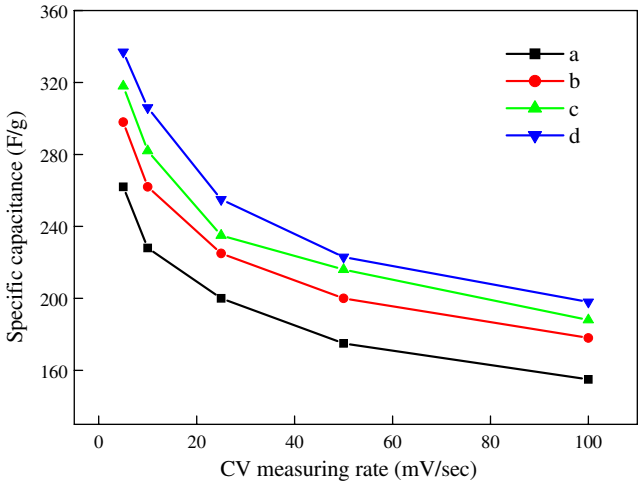

Fig. 4 Specific capacitances of the various electrodes as a function of the measuring CV scan rate. Curves *a–d* represent the Mn oxide potentiodynamically deposited at 100, 200, 300, and 400 mV/s, respectively

factor in determining the capacitive performance. Our previous study [16] proposed that the hydrous state is the most important parameter that governs the specific capacitance of Mn oxide. The analytical results presented in this investigation again support this hypothesis. A highly hydrous state can increase ionic conductivity [23], and thus enhance the activity and utilization of Mn oxide. As a result, the pseudocapacitive properties of the electrode were improved.

The electrochemical stability of the deposited oxide films was also evaluated. Figure 5 shows the variations of the specific capacitance, measured at a CV scan rate of 50 mV/s, with the redox cycle number for the various oxide electrodes. As shown, although the 400-mV/s-deposited oxide had the highest initial capacitance among the electrodes, its decay was more pronounced upon CV cycling. This result suggests that when pursuing a high specific capacitance of Mn oxide by increasing the deposition sweep rate, the relatively quick performance degradation of the electrode should be considered. The capacitance retained ratios after 500 cycles (capacitance at the 500th cycle/capacitance at the first cycle) of the 100-, 200-, 300-, and 400-mV/s-deposited Mn oxides were 84%, 81%, 76%, and 72%, respectively. The inferior cyclic stability of the oxide deposited at the higher potential sweep rate was attributed to the irreversibly cathodic dissolution of Mn oxide, as shown in Fig. 3. Moreover, our previous study [16] also suggested that a more porous electrode would improve the electrochemical reaction homogenization and would also allow for larger volume expansion and contraction of Mn oxide during charging and discharging. Since the created internal stress may be lower, the porous structure could prevent the electrode from physical damage. The better durability of the oxide electrode deposited at a lower sweep rate may also be explained from this aspect.

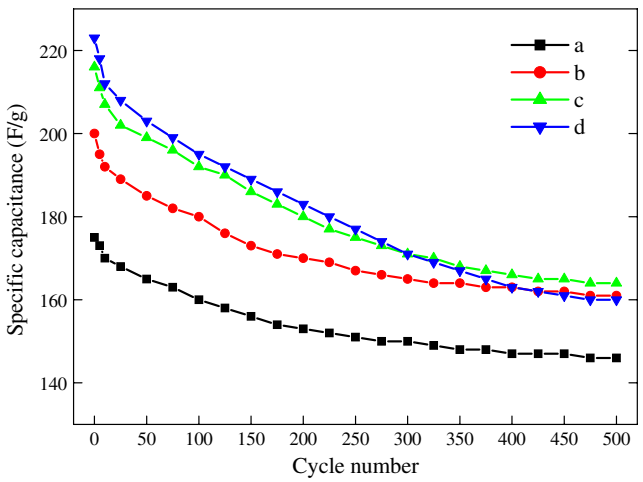

Fig. 5 Variations of the specific capacitance, measured at a CV scan rate of 50 mV/s, with the redox cycle number for the Mn oxide films deposited at various potential sweep rates (*curve a* 100 mV/s, *curve b* 200 mV/s, *curve c* 300 mV/s, *curve d* 400 mV/s)

Conclusions

Potentiodynamic electrodeposition was used to prepare Mn oxide thin film for supercapacitor applications. Adjusting the potential sweep rate for deposition can be used to control the material characteristics of the obtained Mn oxide. A higher potential sweep rate led to a higher hydrous state of the deposited film, which was considered as the most important factor that determined the pseudocapacitive performance of Mn oxide. The oxide-specific capacitance increased from 262 to 337 F/g when the deposition sweep rate was increased from 100 to 400 mV/s. However, a higher deposition sweep rate produced a more compact oxide film with a higher apparent density. This oxide also had a lower Mn valent state and was more easily dissolved in the electrolyte. Therefore, its cyclic stability is inferior to that of the oxide deposited at a lower potential sweep rate. A proper potential sweep rate for electrodeposition should be chosen or an appropriate post-treatment has to be performed before the overall pseudocapacitive performance of the oxide film electrode can be optimized.

Acknowledgments The authors would like to thank the National Science Council of the Republic of China for financially supporting this research (under Contract No. NSC 95-2221-E-006-192).

References

1. Conway BE (1999) Electrochemical supercapacitors. Kluwer-Plenum, New York
2. Pang SC, Anderson MA (2000) J Mater Res 15:2096–2106
3. Hu CC, Tsou TW (2002) Electrochem Comm 4:105–109
4. Toupin M, Brousse T, Bélanger D (2004) Chem Mater 16:3184–3190
5. Chang JK, Lee MT, Tsai WT (2007) J Power Sources 166:590–594
6. Chang JK, Tsai WT (2003) J Electrochem Soc 150:A1333–A1388
7. Lee HY, Manivannan V, Goodenough JB (1999) Comptes Rendus Chimie 2:565–577
8. Lee HY, Goodenough JB (1999) J Solid State Chem 144:220–223
9. Pang SC, Anderson MA, Chapman TW (2000) J Electrochem Soc 147:444–450
10. Reddy RN, Reddy RG (2003) J Power Sources 124:330–337
11. Broughton JN, Brett MJ (2002) J Electrochem Solid-State Lett 5: A279–A282
12. Subramanian V, Zhu H, Vajtai R, Ajayan PM, Wei B (2005) J Phys Chem B 109:20207–20214
13. Chang JK, Chen YL, Tsai WT (2004) J Power Sources 135:344–353
14. Hu CC, Wang CC (2003) J Electrochem Soc 150:A1079–A1084
15. Prasad KR, Miura N (2004) J Power Sources 135:354–360
16. Chang JK, Huang CH, Lee MT, Tsai WT, Deng MJ, Sun IW (2009) Electrochim Acta 54:3278–3284
17. Chen YS, Hu CC, Wu YT (2004) J Solid State Electrochem 8:467–473
18. Chang JK, Hsieh WC, Tsai WT (2008) J Alloys Compd 461:667–674
19. Hasemi T, Brinkman AW (1992) J Mater Res 7:1278–1282
20. Chigane M, Ishikawa M (2000) J Electrochem Soc 147:2246–2251
21. Oku M, Hirokawa K, Ikeda S (1975) J Electron Spectrosc Relat Phenom 7:465–473
22. Chigane M, Ishikawa M, Izaki M (2001) J Electrochem Soc 148: D96–D101
23. Kim H, Popov BN (2003) J Electrochem Soc 150:D56–D62